April 1985 LIDS-P-1450

AN EFFICIENT MAXIMUM ENTROPY TECHNIQUE FOR 2-D ISOTROPIC RANDOM FIELDS

Ahmed H. Tewfik, Bernard C. Levy and Alan S. Willsky

Laboratory for Information and Decision Systems
and the Department of Electrical Engineering and
Computer Science, M.I.T., Cambridge, MA. 02139

Abstract

A new direct method for estimating the power spectrum of two-dimensional isotropic random fields is presented. It is shown that the problem of constructing the maximum entropy estimate of the power spectrum is equivalent to that of estimating the value of the random field at the origin of a disk of observation. An efficient algorithm for the construction of the MEM spectrum estimate with $0(N^2)$ operation (similar to the Levinson recursions in one dimension) is described and illustrated.

This work was supported in part by the National Science Foundation under Grant ECS-83-12921, and in part by the Army Research Office under Grant No. DAAG-29-84-K-0005.

I. INTRODUCTION

The need for efficient power spectrum estimation techniques arises in a number of practical applications, such as speech processing [1], radar [2], sonar [3], image processing [4] and seismic signal processing [5], to mention a few. For one-dimensional signals, the maximum-entropy spectral estimation method (MEM) has become very popular due to the facts that it can provide excellent frequency resolution, and that it can be implemented in a computationally efficient way [6]. Because of the multidimensional nature of the signals arising in some applications (e.g. geophysical problems, imaging, sonar, etc.) a number of maximum entropy algorithms have been developed over the past ten years ([7]-[9]) for estimating two-dimensional spectra. However, all of the proposed two-dimensional MEM algorithms are iterative in nature. The convergence of these algorithms has been observed to be slow in the case of highly peaked spectra. Furthermore, some of the algorithms are not guaranteed to converge [10]. In this paper we present a direct method for finding the maximum entropy estimate of the power spectrum of a two-dimensional isotropic field. Isotropic random fields are characterized by a covariance function which is invariant under all rigid body motions -- i.e. the correlation of the values of the field at two points depends only on the distance between the points. Apart from the fact that the isotropic property is the natural extention of stationarity in one dimension, isotropic fields deserve special attention because they arise in a number of physical problems of interest among which we can mention

the study of sound propagation ([11] chapter 10), the investigation of the temperature and pressure distributions in the atmosphere at a constant altitude [12], and the analysis of turbulence in fluid mechanics [13].

This paper is organized as follows. In Section 2 we develop an expression for the maximum entropy spectral estimate of an isotropic field. In Section 3 the spectral estimation problem is related to the problem of finding a smoothed estimate of an isotropic field given some noisy observations. A fast algorithm developed for the smoothing problem is then presented and used to construct the MEM spectral estimate. The numerical implementation of this fast algorithm is discussed in Section 4 and some examples are given in Section 5.

II. THE MEM SPECTRAL ESTIMATE

Consider the following problem. Let

$$y(\underline{r}) = z(\underline{r}) + v(\underline{r}), \quad \underline{r} \in \mathbb{R}^2 \tag{2.1}$$

be some observations of a two-dimensional isotropic zero-mean Gaussian random field $z(\underline{r})$ with covariance function $K_{zz}(|\underline{r}-\underline{s}|) = E[z(\underline{r})z(\underline{s})]$. Here, $v(\underline{r})$ is a two-dimensional white Gaussian noise of strength one, and is uncorrelated with $z(\underline{r})$. Given the value of the covariance function of $y(\underline{r})$, $K_{yy}(|\underline{r}-\underline{s}|) = E[y(\underline{r})y(\underline{s})]$, for $|r-s| < R$ it is required to determine the "most random" field $y(\cdot)$ whose covariance function is consistent with the set of known values. The above problem can be formulated more precisely as the problem of maximizing the entropy

$$H = \int_{-\infty}^{\infty} \int_{-\infty}^{\infty} df_1 df_2 \ \ell n \ S_{yy}(f_1,f_2) \tag{2.2a}$$

where $S_{yy}(f_1,f_2)$ is the spectrum of $y(\cdot)$, i.e. the 2-D Fourier transform of $K_{yy}(|\underline{r}|)$ viewed as a function of the two-vector $\underline{r}$. Since $K_{yy}(\cdot)$ depends only on $|\underline{r}|$, it is straightforward to show that S_{yy} is actually only a function of $\lambda = (f_1^2+f_2^2)^{1/2}$ [14], and with a slight abuse of notation we will write this as $S_{yy}(\lambda)$. Furthermore, $S_{yy}(\lambda)$ can be shown to be nothing more than the Hankel transform of $K_{yy}(r)$ viewed as a function of the scalar $r = |\underline{r}|$:

$$S_{yy}(\lambda) = \int_0^{\infty} dr \ rJ_0(\lambda r)K_{yy}(r) \quad ,$$

and (2.2a) can then be reduced to

$$H = 2\pi \int_0^{\infty} d\lambda \ \lambda \ \ell n \ S_{yy}(\lambda) \quad . \tag{2.2b}$$

The problem is now to maximize H subject to:

$$\text{(i)} \quad S_{yy}(\lambda) \geq 0 \quad \text{for } \lambda \geq 0 \tag{2.3}$$

and

$$\text{(ii)} \quad \int_0^\infty S_{yy}(\lambda)\, J_0(\lambda r)\lambda d\lambda = K_{yy}(r) \quad , \quad \text{for} \quad r < R \quad . \tag{2.4}$$

Note that we assume here that $K_{yy}(r)$ is known for $r < R$.

By using the approach outlined in [15] for solving optimization problems with global pointwise inequality constraints, we find that the power spectral estimate $\hat{S}_{yy}(\lambda)$ is given by

$$\hat{S}_{yy}(\lambda) = \frac{2\pi}{A(R,\lambda)} \quad , \tag{2.5}$$

where

$$A(R,\lambda) = \int_0^R a(R,r)\, J_0(\lambda r)\, r dr \quad , \tag{2.6}$$

and $a(R,r)$ is the Lagrange multiplier function associated with the constraint (2.4). The spectral estimate $\hat{S}_{yy}(\lambda)$ as given by equation (2.5) is shown in the appendix to satisfy the non-negativity constraint (2.3). Thus, the problem has been reduced to determining $a(R,r)$.

Combining equations (2.4), (2.5) and (2.6) we obtain

$$\int_0^R ds\ s\ a(R,s)k_0(r,s) + \frac{1}{2\pi} a(R,r) = 2\pi \frac{\delta(r)}{r} \quad , \ r < R \tag{2.7}$$

where

$$k_0(r,s) = \int_\Theta^\infty J_0(\lambda r)J_0(\lambda s)S_{zz}(\lambda)\lambda d\lambda \quad , \tag{2.8}$$

and $S_{zz}(\lambda)$ is the Hankel transform of the covariance function $K_{zz}(r)$. The function $k_0(r,s)$ can be interpreted as being the covariance function

of the process $z_0(r)$, $0 \leq r \leq R$, where $z_0(r)$ is the zeroth order Fourier coefficient of $z(\underline{r})$, $\underline{r} = (r \sin \theta, r \cos \theta)$, in the Fourier expansion of $z(\underline{r})$ in terms of the coordinate angle θ [16]. It is assumed here that $k_0(r,s)$ is known over $0 \leq r, s \leq R$, which is a more stringent requirement than knowing $K_{yy}(r)$ or equivalently $K_{zz}(r)$ over $0 \leq r \leq R$, since we have

$$k_0(r,s) = \frac{1}{2\pi} \int_0^{2\pi} d\theta \; K_{zz}((r^2+s^2-2rs \cos \theta)^{1/2}) \; , \tag{2.9}$$

from which it appears that $k_0(r,s)$ depends on $K_{zz}(r)$ for $0 \leq r \leq 2R$. This last interval is twice as long as the one over which $K_{zz}(r)$ is assumed to be known. However, in practice $k_0(r,s)$ is evaluated directly from the observed data $y(\underline{r})$, and it is therefore reasonable to assume that $k_0(r,s)$ is given for $0 \leq r, s \leq R$. Furthermore, let us make two additional comments. The first is that although $z(\underline{r})$ is isotropic, $z_0(r)$ is <u>not</u> a stationary process as a function of the scalar r, i.e. $k_0(r,s)$ is <u>not</u> a function of r-s. Secondly, equations (2.5) - (2.7) imply that the optimal spectral estimate depends only on the second-order statistics of $z_0(r)$, the process obtained by averaging $z(\underline{r})$ along circles centered at the origin.

Instead of dealing with the integral equation (2.7), let us assume that $a(R,r)$ has the form

$$a(R,r) = 4\pi^2 \left(\frac{\delta(r)}{r} - c_0(R,r)\right) \quad 0 \leq r \leq R \; , \tag{2.10}$$

or equivalently that $\hat{S}_{yy}(\lambda)$ has the form

$$\hat{S}_{yy}(\lambda) = \frac{1}{2\pi(1-C_0(R,\lambda))} \tag{2.11}$$

where

$$C_0(R,\lambda) = \int_0^R dr \; r \; J_0(\lambda r) \; c_0(R,r) \; . \tag{2.12}$$

Substituting equation (2.10) into equation (2.7) yields the following integral equation for the unknown $c_0(R,r)$

$$k_0(0,r) = \int_0^R ds\ s\ k_0(r,s)c_0(R,s) + \frac{1}{2\pi} c_0(R,r) \quad , \text{ for } \quad r \leq R \quad . \tag{2.13}$$

Equation (2.13) is quite interesting, for it also arises in the context of smoothing for isotropic random fields [16], as we shall see in the next section. The function $c_0(R,r)$ turns out to be the optimum linear filter for estimating $z(\underline{0})$ given the observations $y(\underline{r})$ on a disk of radius R centered at the origin. A fast algorithm for the construction of $c_0(R,r)$ was developed in [16] and is reviewed in the next section.

III. A FAST ALGORITHM FOR THE CONSTRUCTION OF $A(R,\lambda)$

We begin this section by giving a brief overview of some of the work presented in [16]. Consider again equation (2.1) and assume that we want to find the best estimates of both $z(\underline{0})$ and $z(\underline{R})$ given the observations $y(\underline{r})$ on a disk of radius $R = |\underline{R}|$ centered around the origin. This problem can be solved by expanding each of the processes appearing in equation (2.1) in Fourier series in terms of the coordinate angle θ. The main feature of such an expansion is that the Fourier coefficient processes of different orders are uncorrelated for an isotropic random field. The original two-dimensional estimation problem thus requires only the solution of a sequence of one-dimensional estimation problems corresponding to the measurements

$$y_n(r) = z_n(r) + v_n(r) \qquad 0 \leq r \leq R \tag{3.1}$$

where $y_n(r)$, $z_n(r)$ and $v_n(r)$ are the n^{th} order Fourier coefficients associated with the observations $y(\underline{r})$, the signal $z(\underline{r})$ and the noise $v(\underline{r})$, respectively. The filtered estimate of $z_n(R)$ given $y_n(r)$ for $r \leq R$ can be obtained by passing $y_n(r)$ through a filter with kernel $g_n(R,r)$. Similarly the smoothed estimate $z_0(0) = z(\underline{0})$ given $y_0(r)$ for $r \leq R$ can be constructed by passing $y_0(r)$ through the filter with kernel $c_0(R,r)$, where we have used this notation for the kernel in anticipation of the result alluded to in the previous section.

Note that since

$$z(\underline{r}) = \sum_{n=-\infty}^{+\infty} z_n(r) e^{jn\theta} \tag{3.2}$$

the optimal estimate of $z(\cdot)$ is given by

$$\hat{z}(\underline{r}) = \sum_{n=-\infty}^{\infty} \hat{z}_n(r)\ e^{jn\theta} \tag{3.3}$$

where $\hat{z}_n(r)$ is the best estimate of $z_n(r)$ given $y_n(r)$, $0 \leq r \leq R$. Recall that what we are interested in doing is estimating $z(\underline{0})$ and $z(\underline{R})$ given the data. Clearly $z(\underline{0})$ has a trivial Fourier series decomposition, since the zero radius circle degenerates to a point. Thus, we must have

$$\hat{z}(\underline{0}) = \hat{z}_0(0) = \int_0^R c_0(R,r)y_0(r)rdr \quad . \tag{3.4}$$

Thus the best estimate at the center of the data disk depends only on the average values of the data on circles centered at the origin. For $r > 0$, all of the $z_n(r)$ are non-zero, and we must in principle estimate them all. In particular

$$\hat{z}_n(R) = \int_0^R g_n(R,r)\ y_n(r)rdr \quad . \tag{3.5}$$

The problem we now investigate is the determination of $c_0(R,r)$ and $g_n(R,r)$.

By using the orthogonality property of linear least-squares estimates, we find that the weighting functions $g_n(R,r)$ and $c_0(R,r)$ satisfy the integral equations

$$k_n(r,R) = \int_0^R k_n(r,s)g_n(R,s)sds + \frac{1}{2\pi}\, g_n(R,r) \quad , \tag{3.6}$$

$$k_0(0,r) = \int_0^R k_0(r,s)c_0(R,s)sds + \frac{1}{2\pi}\, c_0(R,r) \quad , \tag{3.7}$$

for $0 \leq r \leq R$, where

$$k_n(r,s) = E[z_n(r)z_n(s)] = \int_0^\infty J_n(\lambda r)J_n(\lambda s)S_{zz}(\lambda)\lambda d\lambda \ , \qquad (3.8)$$

are assumed to be known for $0 \leq r,s \leq R$. Comparing (2.12) and (3.7) we see that our use of the notation $c_0(R,r)$ is justified. Equations (3.6) and (3.7) can be discretized individually and solved seperately for $g_n(R,r)$ and $c_0(R,r)$. However, such an approach requires $0(N^3)$ operations, where N is the number of discretization points at which $g_n(R,r)$ and $c_0(R,r)$ are computed. A more efficient procedure for constructing $g_n(R,r)$ and $c_0(R,r)$ results from using equations (3.6) and (3.7) together with the following coupled partial differential equations [16]:

$$(\frac{\partial}{\partial R} - \frac{n}{R})\ g_n(R,r) + (\frac{\partial}{\partial r} + \frac{n+1}{r})\ g_{n+1}(R,r) = -\rho_n(R)g_n(R,r) \ , \qquad (3.9a)$$

$$(\frac{\partial}{\partial r} - \frac{n}{r})\ g_n(R,r) + (\frac{\partial}{\partial R} + \frac{n+1}{R})\ g_{n+1}(R,r) = \rho_n(R)g_{n+1}(R,r) \ , \qquad (3.9b)$$

$$\frac{\partial}{\partial R}\ c_0(R,r) = -Rc_0(R,R)g_0(R,r) \ , \qquad (3.10)$$

with

$$\rho_n(R) \triangleq R(g_n(R,R) - g_{n+1}(R,R)) \ , \qquad (3.11)$$

and initial conditions

$$\frac{\partial}{\partial r}\ g_0(R,r)\Big|_{r=0} = 0 \ , \qquad (3.12a)$$

$$g_n(R,0) = 0 \ , \quad \text{for } n \neq 0 \qquad (3.12b)$$

$$c_0(0,r) = K_{zz}(r) \ . \qquad (3.12c)$$

Equations (3.9) - (3.11) can be derived by exploiting the special structure of $k_n(r,s)$ as displayed by equation (3.8), and by using the properties of Bessel functions. Our primary interest now is in computing $c_0(R,r)$. Examining (3.9) - (3.12) we see that by specializing (3.9) to n=0 only, we obtain a set of coupled equations for $g_0(R,r)$, $g_1(R,r)$ and $c_0(R,r)$. It is these equations that we will solve. Note also that by using the above mentioned coupled partial differential equations, one can compute $c_0(R,r)$ recursively as a function of R so that the spectral estimate $\hat{S}_{yy}(\lambda)$ can be easily updated whenever new measurements become available -- i.e. as the disk radius R is increased. In this respect equations (3.9) - (3.11) are similar to the Levinson equations of one-dimensional linear prediction. Once $c_0(R,r)$ becomes available, its Hankel transform $C_0(R,\lambda)$ can be obtained easily by using any of the existing fast Hankel transform techniques (see [17]).

IV. NUMERICAL IMPLEMENTATION

For the case where n=0, the system (3.9) can be rewritten as

$$\frac{\partial}{\partial R}\ g_0(R,r) + \left(\frac{\partial}{\partial r} + \frac{1}{r}\right) g_1(R,r) = -\rho_0(R)\, g_0(R,r)\ , \tag{4.1a}$$

$$\frac{\partial}{\partial r}\ g_0(R,r) + \left(\frac{\partial}{\partial R} + \frac{1}{R}\right) g_1(R,r) = \rho_0(R)\, g_1(R,r)\ , \tag{4.1b}$$

where these equations are subject to (3.11) - (3.12) and must be solved for $r \leq R$ and $0 \leq R \leq R_*$, where R_* is the disk radius beyond which $K_{yy}(r)$ needs to be extended. The system (4.1) constitutes a quasilinear hyperbolic system [18] with characteristics given by

$$\frac{dR}{dr} = \pm 1\ . \tag{4.2}$$

We shall now apply the method of characteristics [18], [19] to solve this system. Specifically we consider a new coordinate system α,β where

$$\alpha = R+r \tag{4.3a}$$

$$\beta = R-r\ . \tag{4.3b}$$

Equations (4.1) can now be rewritten in the new coordinate system as

$$\frac{\partial}{\partial \alpha}\ g_0(\alpha,\beta) + \frac{\partial}{\partial \alpha}\ g_1(\alpha,\beta) = -\rho_0\left(\frac{\alpha+\beta}{2}\right) g_0(\alpha,\beta) + \left(\rho_0\left(\frac{\alpha+\beta}{2}\right) - \frac{4\alpha}{(\alpha^2-\beta^2)}\right) g_1(\alpha,\beta) \tag{4.4a}$$

$$\frac{\partial}{\partial\beta} g_0(\alpha,\beta) - \frac{\partial}{\partial\beta} g_1(\alpha,\beta) = -\rho_0\left(\frac{\alpha+\beta}{2}\right) g_0(\alpha,\beta)$$

$$- \left(\rho_0\left(\frac{\alpha+\beta}{2}\right) + \frac{4\beta}{\alpha^2-\beta^2}\right) g_1(\alpha,\beta) \quad . \qquad (4.4b)$$

Note that in the new coordinate system each partial differential equation involves differentiation with respect to only one of the independent variables α and β. Thus, to compute $g_0(R,r)$ and $g_1(R,r)$ within the domain of influence of an initial data segment, we can integrate equations (4.4) along the characteristic direction α = constant (for (4.4b)) and β = constant (for (4.4a)) (or equivalently along lines of slope $\pm$ 45° in the (R,r) plane), as shown in Fig. 1. The domain of influence of a point (R_0,r_0) is the set of points (R,r) at which the solution is influenced by the initial data at the point (R_0,r_0). For example, if the values of $g_0(R,r)$ and $g_1(R,r)$ have been computed inside the triangle OAB (see Fig. 1), and in particular on the line AB, then by integrating equation (4.4a) along β = constant lines starting on AB, we can compute the sum $g_0(R,r) + g_1(R,r)$ inside the parallelogram ABGF. Similarly, by integrating (4.4b) along α = constant directions starting on AB, we can compute the difference $g_0(R,r) - g_1(R,r)$ inside the region ABED. Thus, $g_0(R,r)$ and $g_1(R,r)$ can be uniquely determined within the triangle ABC (the intersection of regions ABED and ABGF). The values of $g_0(R,r)$ and $g_1(R,r)$ which are outside triangle ABC, will have to be computed using integral equations (3.6) and (3.7).

Our numerical procedure is based on equations (3.6) - (3.7), (3.10) and (4.4). We divide the interval [0,R*] into N subintervals of length Δ = R*/N. Denoting $G_n(k,\ell) = g_n(k\Delta,\ell\Delta)$ and $C_0(k,\ell) = c_0(k\Delta,\ell\Delta)$, if at

stage k we assume that $G_0(k,\ell)$, $G_1(k,\ell)$ and $C_0(k,\ell)$ have been computed for $0 \leq \ell \leq k$ (i.e. on the line AB of Fig. 1), then $G_0(k+1,\ell)$, $G_1(k+1,\ell)$ and $C_0(k+1,\ell)$ can be evaluated for $0 < \ell \leq k+1$ by integrating equations (4.4) along the characteristic directions R = constant $\pm r$ for G_0 and G_1, and by integrating (3.10) along r = constant for C_0. For $\ell = k, k+1$ (i.e. outside of the triangle ABC), $G_0(k+1,\ell)$, $G_1(k+1,\ell)$ and $C_0(k+1,\ell)$ can be computed by solving three two by two linear systems obtained by discretizing integral equations (3.6) and (3.7) (see Fig. 1). If we use a simple Euler difference method to integrate (4.4) and (3.10), and solving for $G_0(k+1,\ell)$ and $G_1(k+1,\ell)$, we obtain the following recursions for $0 < \ell \leq k-1$,

$$G_0(k+1,\ell) = \frac{(a_1 b_2 - a_2 b_1)}{a_3(a_1-a_2)} \quad , \tag{4.5}$$

$$G_1(k+1,\ell) = \frac{(b_1-b_2)}{(a_1-a_2)} \quad , \tag{4.6}$$

$$b_1 = G_0(k,\ell-1) + G_1(k,\ell-1) + \rho(k)\Delta \frac{(G_1(k,\ell-1)-G_0(k,\ell-1))}{\sqrt{2}} - \left(\frac{1}{k} + \frac{1}{\ell-1}\right) \frac{G_1(k,\ell-1)}{\sqrt{2}} \tag{4.7}$$

$$b_2 = G_0(k,\ell+1) - G_1(k,\ell+1) + \left(\frac{1}{\ell+1} - \frac{1}{k}\right) \frac{G_1(k,\ell+1)}{\sqrt{2}} - \rho(k)\Delta \frac{(G_1(k,\ell+1) + G_0(k,\ell+1))}{\sqrt{2}} \quad , \tag{4.8}$$

$$a_1 = 1 + \frac{1}{\sqrt{2}} \left(\frac{1}{k+1} + \frac{1}{\ell} - \rho(k)\Delta \right) , \tag{4.9}$$

$$a_2 = -1 + \frac{1}{\sqrt{2}} \left(\frac{1}{k+1} - \frac{1}{\ell} + \rho(k)\Delta \right) , \tag{4.10}$$

$$a_3 = 1 + \frac{\rho(k)\Delta}{\sqrt{2}} , \tag{4.11}$$

$$\rho(k) = k\Delta \left(G_0(k,k) - G_1(k,k) \right) , \tag{4.12}$$

$$C_0(k+1,\ell) = C_0(k,\ell) - k\Delta^2 C_0(k,k) G_0(k,\ell) . \tag{4.13}$$

Similarly, if we discretize equations (3.6) and (3.7) using the trapezoidal rule, we obtain for ℓ=k, k+1

$$\begin{aligned} \frac{1}{2\pi} G_n(k+1,\ell) &= k_n((k+1)\Delta, \ell\Delta) \\ &\quad - \sum_{i=1}^{k} k_n(\ell\Delta, i\Delta) G_n(k+1,i) i\Delta^2 \\ &\quad - k_n(\ell\Delta, (k+1)\Delta) G_n(k+1, k+1) \frac{(k+1)\Delta^2}{2} \end{aligned}$$

$$n = 0,1 , \tag{4.14}$$

$$\begin{aligned} \frac{1}{2\pi} C_0(k+1,\ell) &= k_0(0,\ell\Delta) \\ &\quad - \sum_{i=1}^{k} k_0(\ell\Delta, i\Delta) C_0(k+1,i) i\Delta^2 \\ &\quad - k_0(\ell\Delta, (k+1)\Delta) C_0(k+1, k+1) (k+1) \frac{\Delta^2}{2} . \end{aligned} \tag{4.15}$$

Other integration rules can be used as well instead of the ones we have chosen. Note that our algorithm involves only numerical integration of ordinary differential equations

and thus can be implemented in a well behaved, stable and convergent manner. Furthermore, it can be checked that this approach requires $0(N^2)$ operations. Recalling that fast Hankel transform algorithms require $0(N \log(N))$ operations [17], we see that the construction of the spectral estimate requires $0(N^2)$ operation and its complexity is of the same order as that of the one-dimensional MEM algorithm.

The procedure for computing the power spectrum can therefore be summarized as follows.

1) From the given data, estimate $K_{yy}(r)$ for $0 \leq r \leq R$, and $k_0(r,s)$ and $k_1(r,s)$ for $0 \leq r,s \leq R$, which are respectively the covariances of the zeroth and first order Fourier processes associated with the signal.

2) Use a discretized form of equations (3.6), (3.7), (3.10) and (4.4), such as equations (4.5) - (4.15), to compute $c_0(R,r)$ recursively.

3) Evaluate the Hankel transform $C_0(R,\lambda)$ of $c_0(R,r)$ by using a fast Hankel transform method.

4) Obtain the spectral estimate as

$$\hat{S}_{yy}(\lambda) = \frac{1}{2\pi(1-C_0(R,\lambda))} \quad .$$

V. EXAMPLES

In this section, we discuss various examples to which our fast algorithm was applied to obtain the maximum entropy estimate of the power spectrum.

Example 1: Consider a covariance function of the form

$$K_{yy}(r) = 8J_0(8r) + 10J_0(13r) + 4J_0(24r) + \frac{1}{2\pi r}\,\delta(r), \qquad (5.1)$$

with corresponding power spectrum

$$S_{yy}(\lambda) = \frac{1}{2\pi} + 8\delta(\lambda-8) + 10\delta(\lambda-13) + 4\,\delta(\lambda-24) \quad . \qquad (5.2)$$

The spectral estimate obtained by assuming that we are given ten equally spaced values of $K_{yy}(r)$ on the interval [0,1] is shown in Figure 2. The algorithm clearly uncovers the impulses at their correct location and is able to resolve the impulses at 8 and 13 rad/sec. A spurious bump occurs near the origin and is due to the finite extent of our original data. With ten equally spaced samples of $K_{yy}(r)$ on the larger interval [0,2] the algorithm yields a much better resolution of the impulses (Fig. 3) and the bump at the origin becomes negligible. However, a peak now appears at a frequency slightly below 21 rad/sec.

Note that 21 rad/sec is equal to the sum of 13 rad/sec and 8 rad/sec. This observation leads us to suspect the presence of a nonlinear effect in our algorithm giving rise to the harmonic at 21 rad/sec. In fact, as in the one-dimensional case, the maximum entropy method is better suited to estimating smooth spectra as can be seen in the next example.

A Pisarenko type procedure will probably be better behaved when the covariance function is equal to a sum of Bessel functions of the zeroth order, which corresponds to the case when the spectrum $S_{yy}(\lambda)$ is constituted of pure lines with a white noise (flat spectrum) background.

Example 2: Consider now a covariance function of the form

$$K_{yy}(r) = 20rK_1(5r) + \frac{1}{2\pi}\frac{\delta(r)}{r}, \tag{5.3}$$

with power spectrum

$$S_{yy}(\lambda) = \frac{200}{(\lambda^2+25)^2} + \frac{1}{2\pi} \quad , \tag{5.4}$$

which is plotted in Figure 4. The estimated spectrum given ten equidistant values of $K_{yy}(r)$ on the interval [0,1] is shown in Figure 5. Note that the spectral estimate we obtain is excellent in spite of the small number of known covariance values.

Example 3: In this last example we apply our algorithm to a covariance function of the form

$$K_{yy}(r) = 20rK_1(10r) + J_0(15r) + \frac{1}{2\pi r}\delta(r), \tag{5.3}$$

where the corresponding power spectrum

$$S_{yy}(\lambda) = \frac{400}{(\lambda^2+100)^2} + \delta(\lambda-15) + \frac{1}{2\pi} \tag{5.4}$$

has a smooth part and an impulse as indicated in Figure 6. The estimated power spectrum given ten values of $K_{yy}(r)$ equally spaced on the interval [0,0.6] is shown in Figure 7. The smooth part is clearly displayed while

the impulse is replaced by a bump centered at the correct impulse location. With thirty equally spaced samples of $K_{yy}(r)$ on the larger interval [0,3] (Fig. 8) the algorithm identifies the impulse at its correct location. However, ripples are now superimposed on the smooth part and are due to some interference effect. Once again the behavior of our algorithm is reminiscent of the behavior of MEM in the 1D case. These experimental results and others we have obtained indicate that the spectral estimates obtained via the technique we propose, depend strongly on the size of the interval on which $K_{yy}(r)$ is known and depend much more weakly on the number of samples that are taken within the interval.

VI. CONCLUSION

In this paper we have presented a direct and fast ($O(N^2)$) method for the evaluation of the MEM estimate of the power spectrum of an isotropic random field in additive white Gaussian noise. The success of this method is predicated on the fact that one can come up with reasonably accurate estimates of $K_{zz}(r)$ (and hence of $k_0(r,s)$ and $k_1(r,s)$) and of the intensity of the two-dimensional white noise process. Further studies might be required in this area. It would also be desirable to obtain a "digital" signal processing theory for isotropic fields based on a theory of sampling for these fields, and to redevelop the above method in a completely discrete setting.

APPENDIX

Proof of the Non-Negativity of the Spectral Estimate $\hat{S}_{yy}(\lambda)$

We will show in this appendix that $C_0(R,\lambda)$ as defined by equations (2.10) and (2.12) satisfies the inequality constraint

$$|C_0(R,\lambda)| < 1, \quad \forall\ \lambda \geq 0 \ . \tag{A.1}$$

Combining this result with equation (2.11) it follows that $\hat{S}_{yy}(\lambda)$ is non-negative for all values of λ.

From equations (2.9) and (2.13), we have

$$k_0(0,r) = K_{zz}(r) = \int_0^R ds\ s\ k_0(r,s)c_0(R,s) + \frac{1}{2\pi}\ c_0(R,r) \tag{A.2}$$

for $r \leq R$. Let

$$c_0(R,r) \triangleq 0 \qquad \text{for } r \geq R \ ,$$

and define a new function $e_0(R,r)$ by the following integral equation

$$K_{z\dot{z}}(r) = \int_0^R ds\ s\ k_0(r,s)\ e_0(R,s) + \frac{1}{2\pi}\ e_0(R,r) \qquad \forall r \geq 0, \tag{A.3}$$

with

$$e_0(R,r) = c_0(R,r) + d_0(R,r) \tag{A.4}$$

and

$$d_0(R,r) = 0 \qquad \text{for } r \leq R \ . \tag{A.5}$$

Clearly,

$$c_0(R,r) = e_0(R,r) \cdot p_R(r), \tag{A.6}$$

where

$$p_R(r) = \begin{cases} 1 & r<R \\ 0 & r>R \end{cases} \tag{A.7}$$

By multiplying both sides of equation (A.3) by $rJ_0(\lambda r)$, and integrating the resulting equation from 0 to infinity, we obtain

$$E_0(R,\lambda) = \frac{S_{zz}(\lambda)}{S_{zz}(\lambda) + \frac{1}{2\pi}} , \tag{A.8}$$

where $E_0(R,\lambda)$ is the Hankel transform of $e_0(R,r)$. Equation (A.8) together with equation (A.6) imply that ([14])

$$C_0(R,\lambda) = \frac{1}{2\pi} \int_0^{\infty} d\lambda' \int_0^{2\pi} d\theta \, \lambda' \frac{S_{zz}(\Lambda)}{S_{zz}(\Lambda)+\frac{1}{2\pi}} \cdot \frac{R\, J_1(R\lambda')}{\lambda'} , \tag{A.9}$$

where

$$\Lambda^2 = \lambda^2 + \lambda'^2 - 2\lambda\lambda'\cos\theta, \tag{A.10}$$

and where $R\,\frac{J_1(R\lambda)}{\lambda}$ is the Hankel transform of $P_R(r)$. Since $S_{zz}(\lambda)$ is a power spectrum then

$$0 < \frac{S_{zz}(\Lambda)}{S_{zz}(\Lambda) + \frac{1}{2\pi}} < 1 \quad . \tag{A.11}$$

Hence

$$|C_0(R,\lambda)| < \frac{1}{2\pi} \int_0^{\infty} d\lambda' \int_0^{2\pi} d\theta\ \lambda' \frac{RJ_1(R\lambda')}{\lambda'} , \tag{A.12}$$

or

$$|C_0(R,\lambda)| < 1 , \tag{A.13}$$

where we have used the fact that

$$\int_0^{\infty} d\lambda\ RJ_1(R\lambda) = P_R(0) = 1 . \tag{A.14}$$

It follows from (A.13) and (2.10) that

$$\hat{S}_{yy}(\lambda) = \frac{1}{2\pi(1-C_0(R,\lambda))} > 0 . \tag{A.15}$$

REFERENCES

[1] J. Makhoul, "Spectral analysis of speech by linear prediction," IEEE Trans. Audio Electroacoust., Vol. AU-21, pp. 140-148, June 1973.

[2] J.H. McClellan and R.J. Purdy, "Applications of digital signal processing to radar," in Applications of Digital Signal Processing, A.V. Oppenheim, Ed., Prentice-Hall, Englewood Cliffs, N.J., 1978.

[3] A.B. Baggeroer, "Sonar signal processing," in Applications of Digital Signal Processing, A.V. Oppenheim, Ed., Prentice-Hall, Englewood Cliffs, N.J., 1978.

[4] S.J. Wernecke and L.R. D'Addario, "Maximum Entropy image reconstruction," IEEE Trans. Comput., Vol. C-26, pp. 351-364, April 1977.

[5] E.A. Robinson and S. Treitel, "Maximum entropy and the relationship of the partial autocorrelation to the reflection coefficients of a layered system," IEEE Trans. Acoustics, Speech and Signal Processing, Vol. ASSP-28, No. 2, pp. 224-235, April 1980.

[6] S.M. Kay and S.L. Marple, "Spectrum analysis - a modern perspective," Proc. IEEE, Vol. 69, No. 11, pp. 1380-1419, Nov. 1981.

[7] S.E. Roucos and D.G. Childers, "A two-dimensional maximum entropy spectral estimator," IEEE Trans. Inform. Theory, Vol. IT-26, pp. 554-560, Sept. 1980.

[8] J.S. Lim and N.A. Malik, "A new algorithm for two-dimensional maximum entropy power spectrum estimation," IEEE Trans. Acoustics, Speech and Signal Processing, Vol. ASSP-29, pp. 401-413, June 1981.

[9] A.K. Jain and S. Raganath, "Two-dimensional spectral estimation," in Proc. RADC Spectrum Estimation Workshop, Rome, N.Y., May 1978, pp. 217-225.

[10] J.H. McClellan, "Multidimensional spectral estimation," Proc. IEEE, Vol. 70, pp. 1029-1039, Sept. 1982.

[11] N.S. Burdic, Underwater Acoustic System Analysis, Prentice Hall Inc., Englewood Cliffs, N.J., 1984.

[12] P.R. Julian and A. Cline, "The direct estimation of spatial wavenumber spectra of atmospheric variables," Jour. Atmospheric Sci., Vol. 31, pp. 1526-1539, 1976.

[13] A.S. Monin and A.M. Yaglom, Statistical Fluid Mechanics: Mechanics of Turbulence, Volume 2, MIT Press, Cambridge, MA., 1975.

[14] A. Papoulis, Systems and Transforms with Applications in Optics, McGraw-Hill, New York, N.Y., 1968.

[15] D.R. Smith, Variational Methods in Optimization, Prentice-Hall, Inc., Englewood Cliffs, N.J., 1974.

[16] B.C. Levy and J.N. Tsitsiklis, "A fast algorithm for linear estimation of two-dimensional isotropic random fields," Report LIDS-P-1192, Laboratory for Information and Decision Systems, MIT, Cambridge, MA., Jan. 1985; also to appear in IEEE Trans. Inform. Theory, Sept. 1985.

[17] D.R. Mook, "An algorithm for the numerical evaluation of the Hankel and Abel transforms," IEEE Trans. on Acoustics, Speech and Signal Processing, Vol. ASSP-31, pp. 979-985, August 1983.

[18] L. Lapidus and G.F. Pinder, Numerical Solution of Partial Differential Equations in Science and Engineering, John Wiley, New York, N.Y., 1982.

[19] W.F. Ames, Numerical Methods for Partial Differential Equations, Academic Press, New York, N.Y., 1977.

FIGURE CAPTIONS

Fig. 1. Discretization scheme and numerical implementation of the recursions for $g_0(R,r)$ and $g_1(R,r)$.

Fig. 2. Spectral estimate for Example 1 when $K_{yy}(r)$ is given on the interval [0,1].

Fig. 3. Spectral estimate for Example 1 when $K_{yy}(r)$ is given on the interval [0,2].

Fig. 4. True spectrum for Example 2.

Fig. 5. Spectral estimate for Example 2 when $K_{yy}(r)$ is given on the interval [0,1].

Fig. 6. True spectrum for Example 3.

Fig. 7. Spectral estimate for Example 3 when $K_{yy}(r)$ is given on the interval [0,0.6].

Fig. 8. Spectral estimate for Example 3 when $K_{yy}(r)$ is given on the interval [0,3].

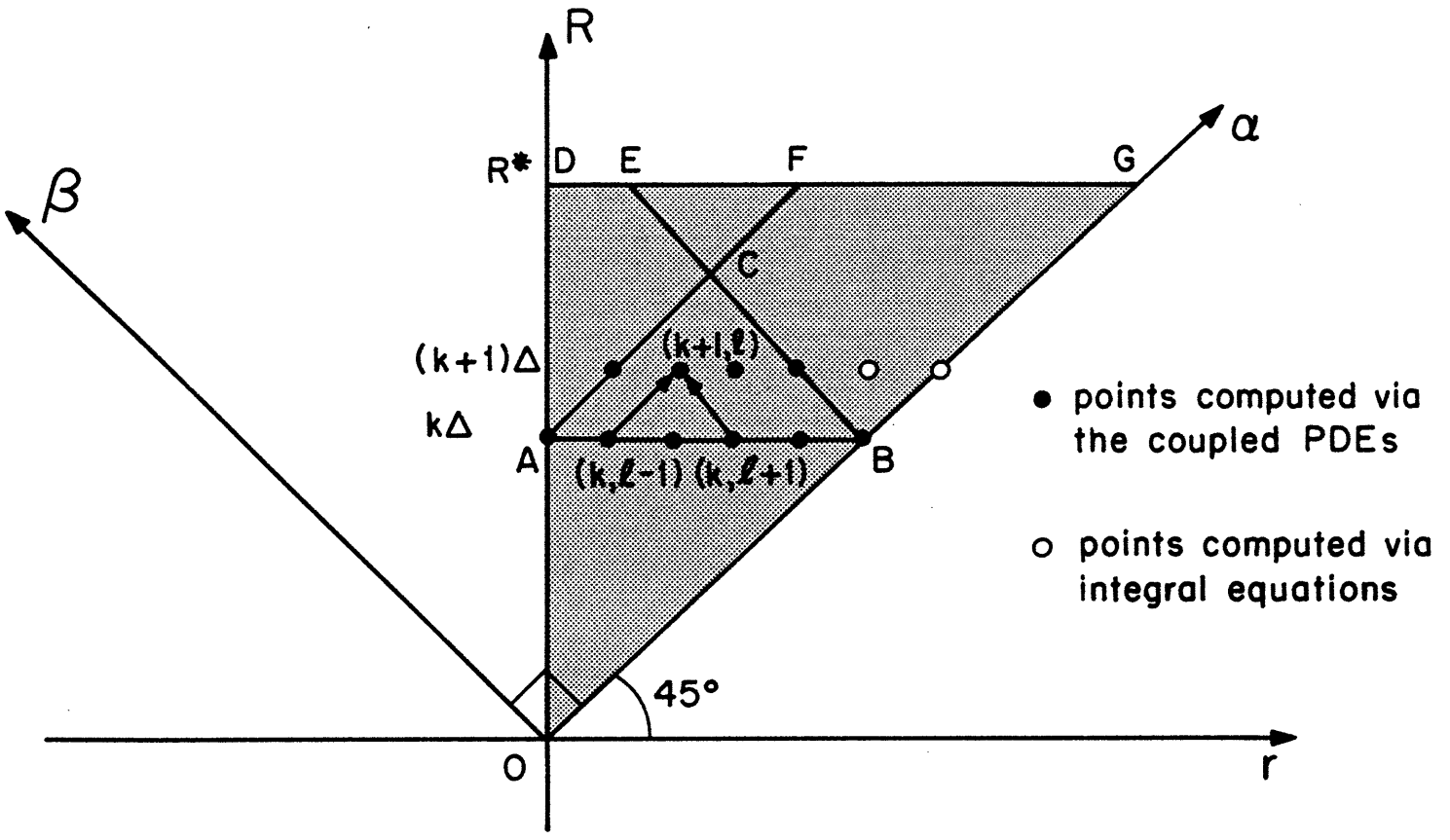
R
α
β
R*
D
E
F
G
C
(k+1)Δ
kΔ
(k+1,ℓ)
A
(k,ℓ-1)
(k,ℓ+1)
B
45°
0
r
• points computed via the coupled PDEs
o points computed via integral equations

Figure 1

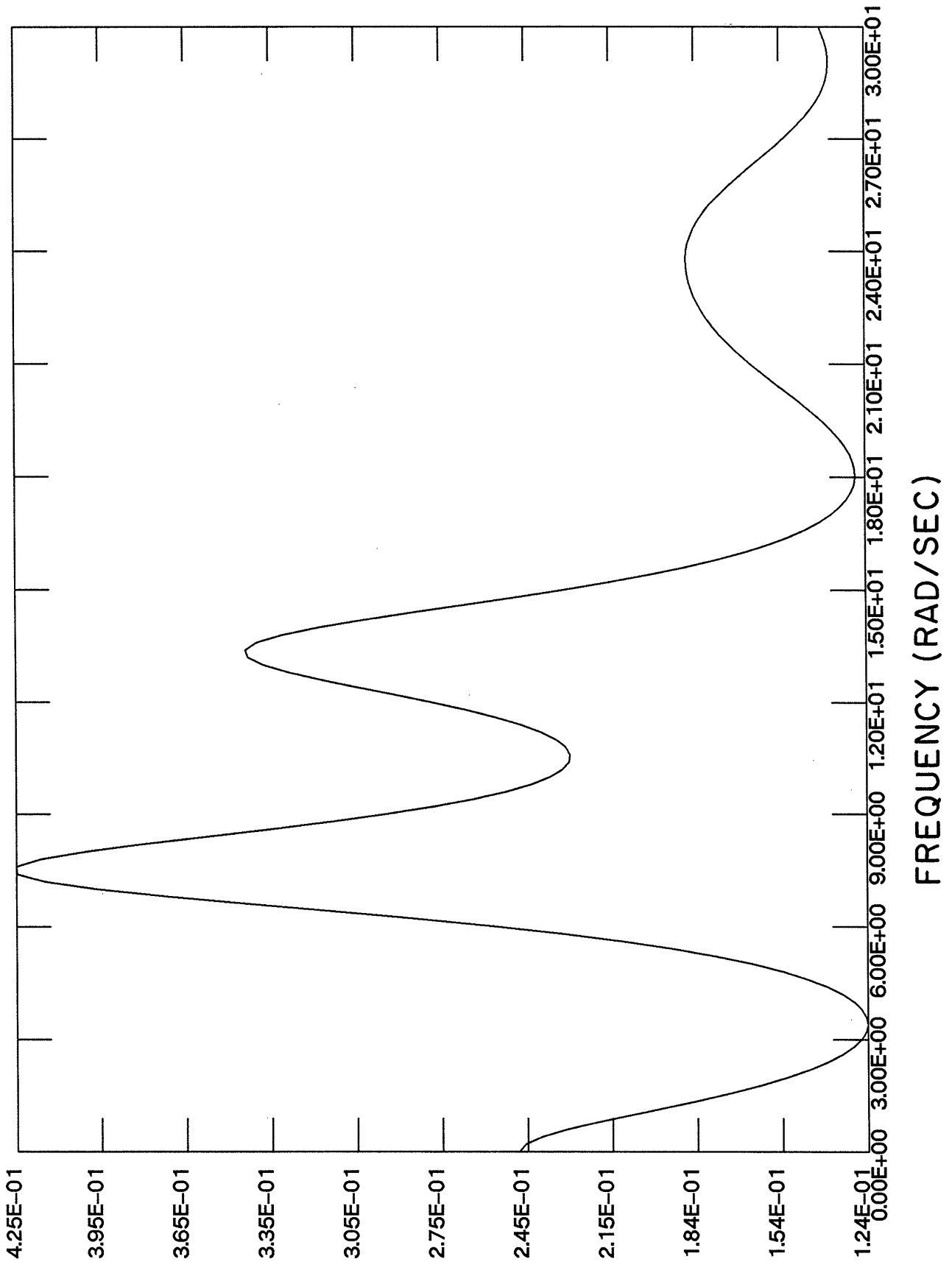
POWER
4.25E-01
3.95E-01
3.65E-01
3.35E-01
3.05E-01
2.75E-01
2.45E-01
2.15E-01
1.84E-01
1.54E-01
1.24E-01
0.00E+00
3.00E+00
6.00E+00
9.00E+00
1.20E+01
1.50E+01
1.80E+01
2.10E+01
2.40E+01
2.70E+01
3.00E+01
FREQUENCY (RAD/SEC)

Figure 2

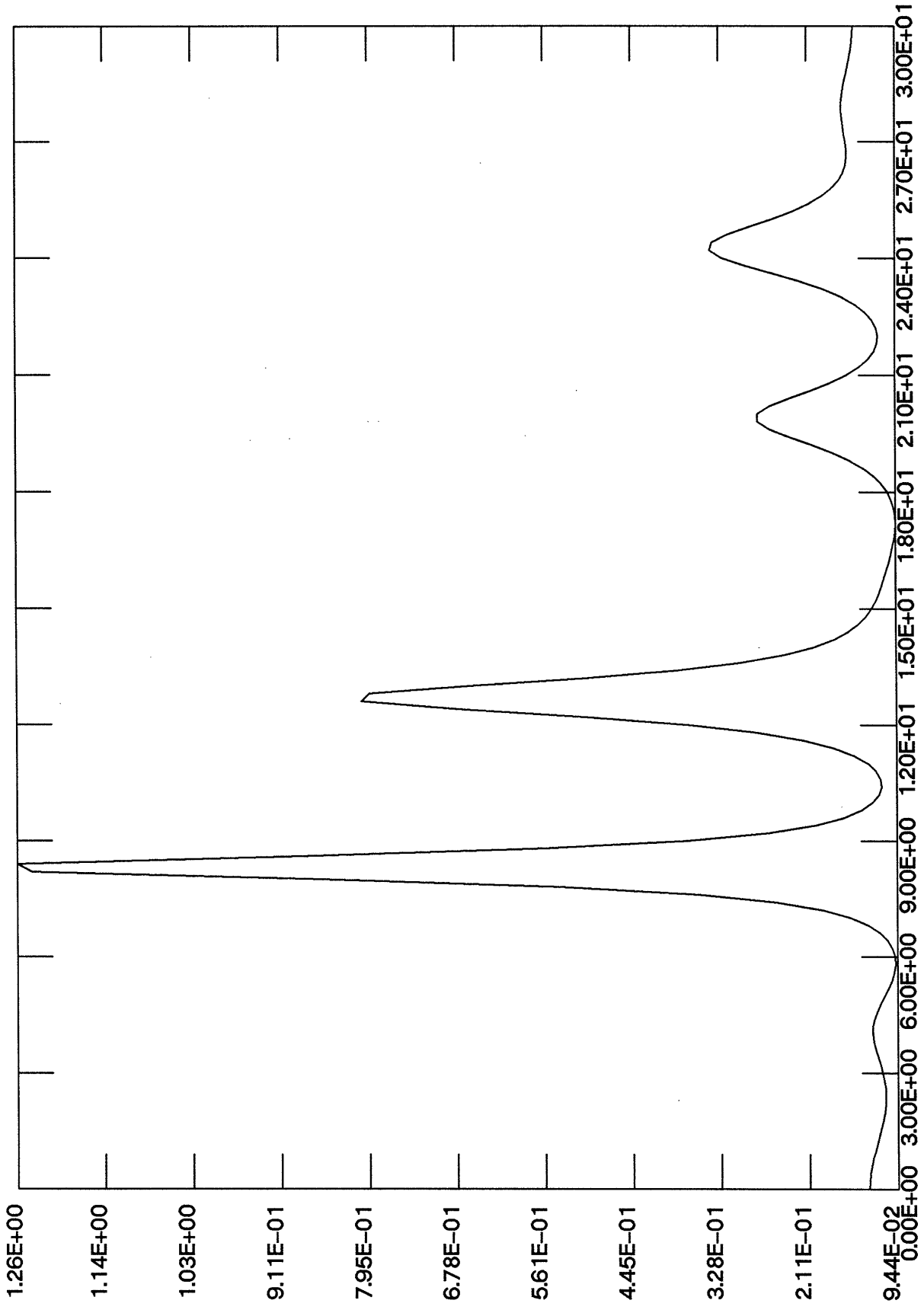
POWER
1.26E+00
1.14E+00
1.03E+00
9.11E-01
7.95E-01
6.78E-01
5.61E-01
4.45E-01
3.28E-01
2.11E-01
9.44E-02
0.00E+00
3.00E+00
6.00E+00
9.00E+00
1.20E+01
1.50E+01
1.80E+01
2.10E+01
2.40E+01
2.70E+01
3.00E+01
FREQUENCY (RAD/SEC)

Figure 3

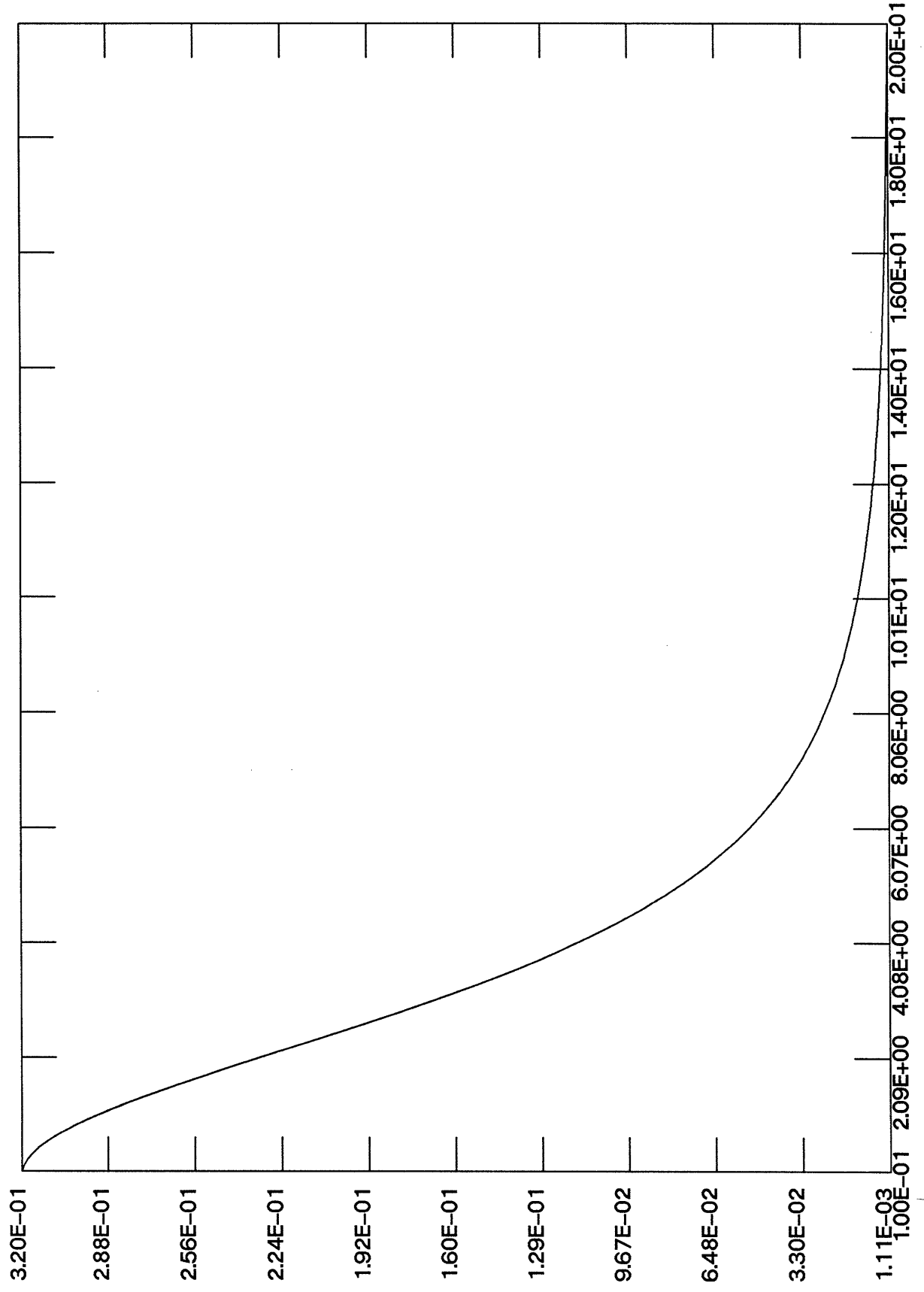
POWER
3.20E-01
2.88E-01
2.56E-01
2.24E-01
1.92E-01
1.60E-01
1.29E-01
9.67E-02
6.48E-02
3.30E-02
1.11E-03
1.00E-01
2.09E+00
4.08E+00
6.07E+00
8.06E+00
1.01E+01
1.20E+01
1.40E+01
1.60E+01
1.80E+01
2.00E+01
FREQUENCY (RAD/SEC)

Figure 4

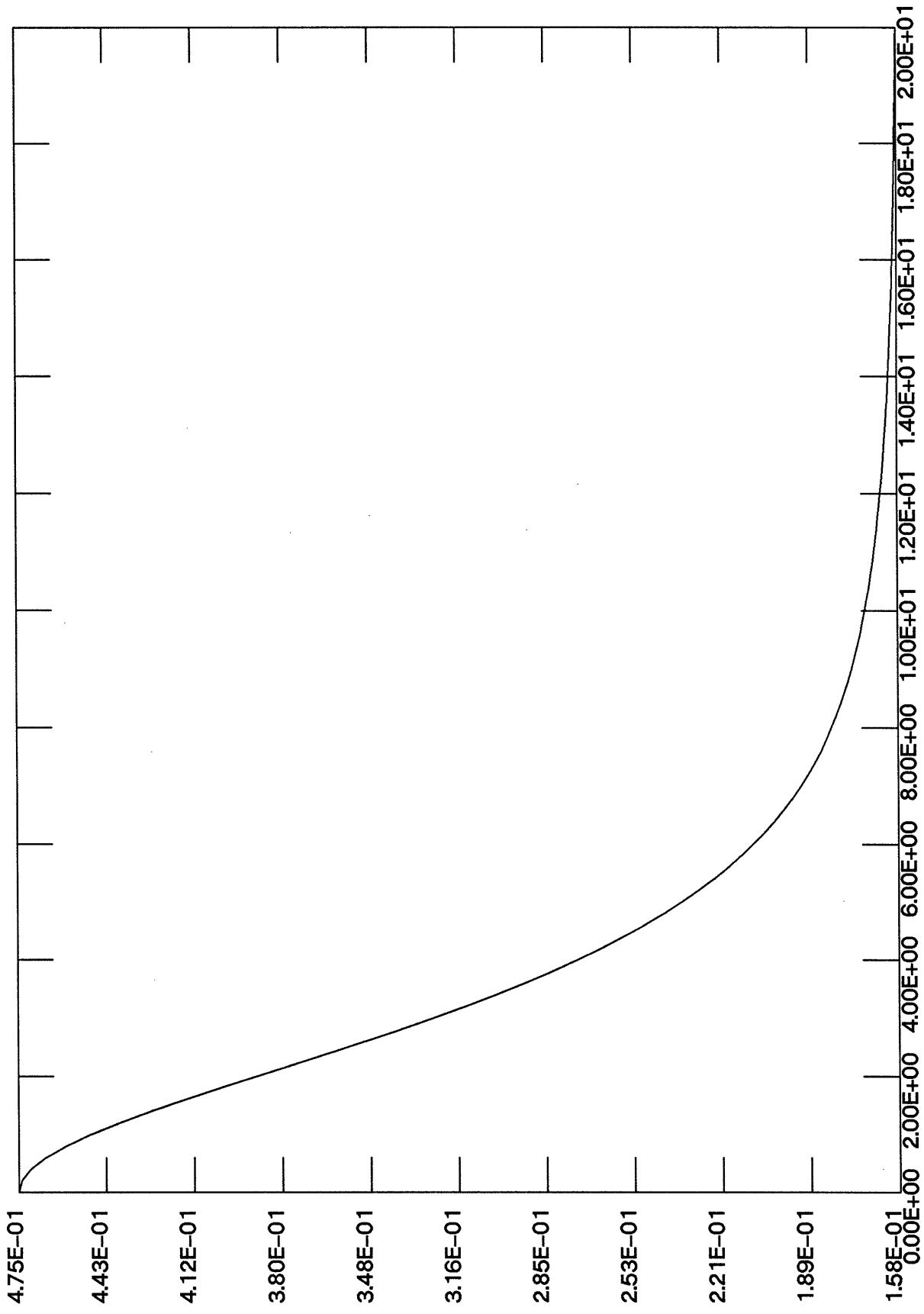
POWER
4.75E-01
4.43E-01
4.12E-01
3.80E-01
3.48E-01
3.16E-01
2.85E-01
2.53E-01
2.21E-01
1.89E-01
1.58E-01
0.00E+00
2.00E+00
4.00E+00
6.00E+00
8.00E+00
1.00E+01
1.20E+01
1.40E+01
1.60E+01
1.80E+01
2.00E+01
FREQUENCY (RAD/SEC)

Figure 5

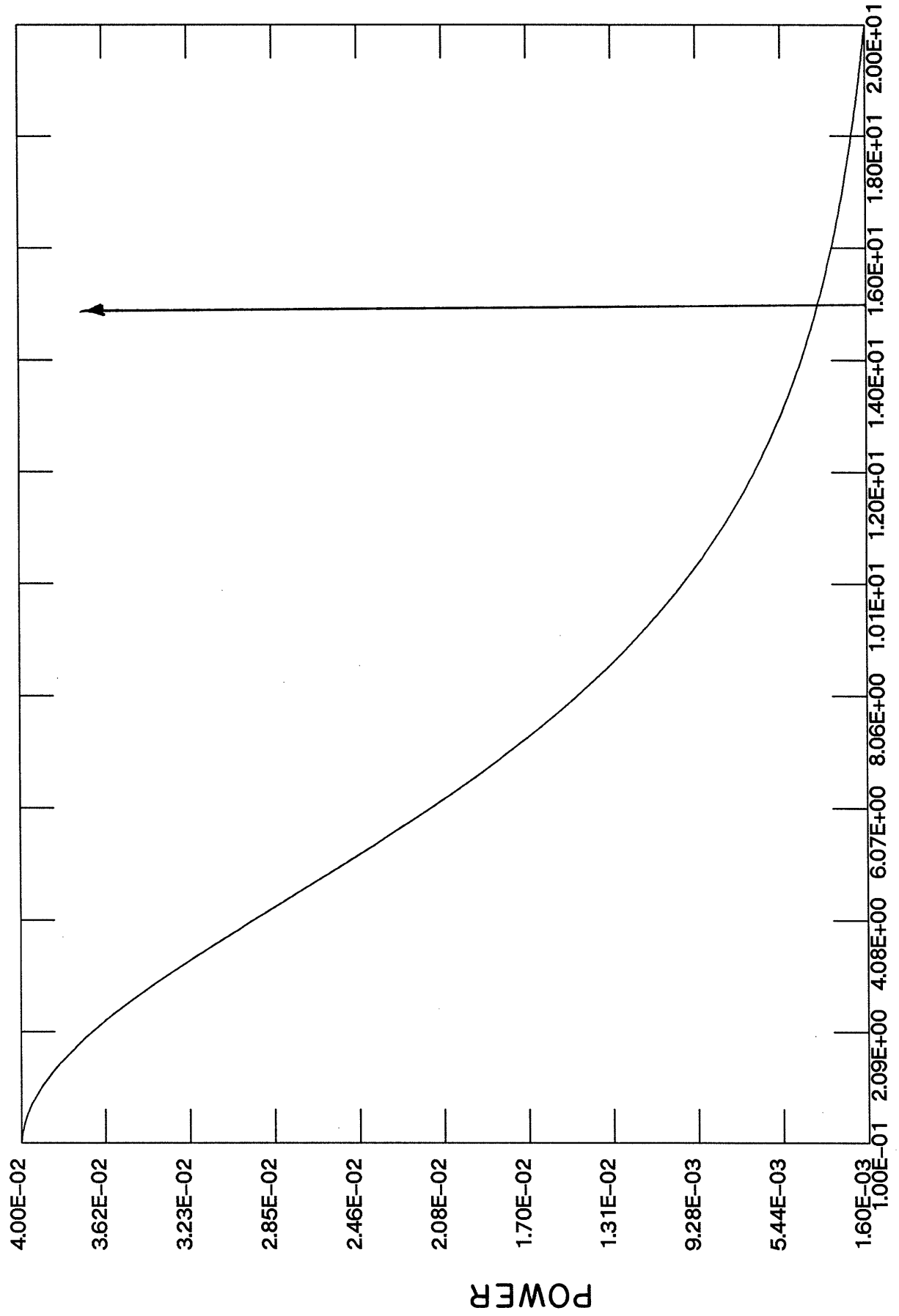
POWER
4.00E-02
3.62E-02
3.23E-02
2.85E-02
2.46E-02
2.08E-02
1.70E-02
1.31E-02
9.28E-03
5.44E-03
1.60E-03
1.00E-01
2.09E+00
4.08E+00
6.07E+00
8.06E+00
1.01E+01
1.20E+01
1.40E+01
1.60E+01
1.80E+01
2.00E+01
FREQUENCY (RAD/SEC)

Figure 6

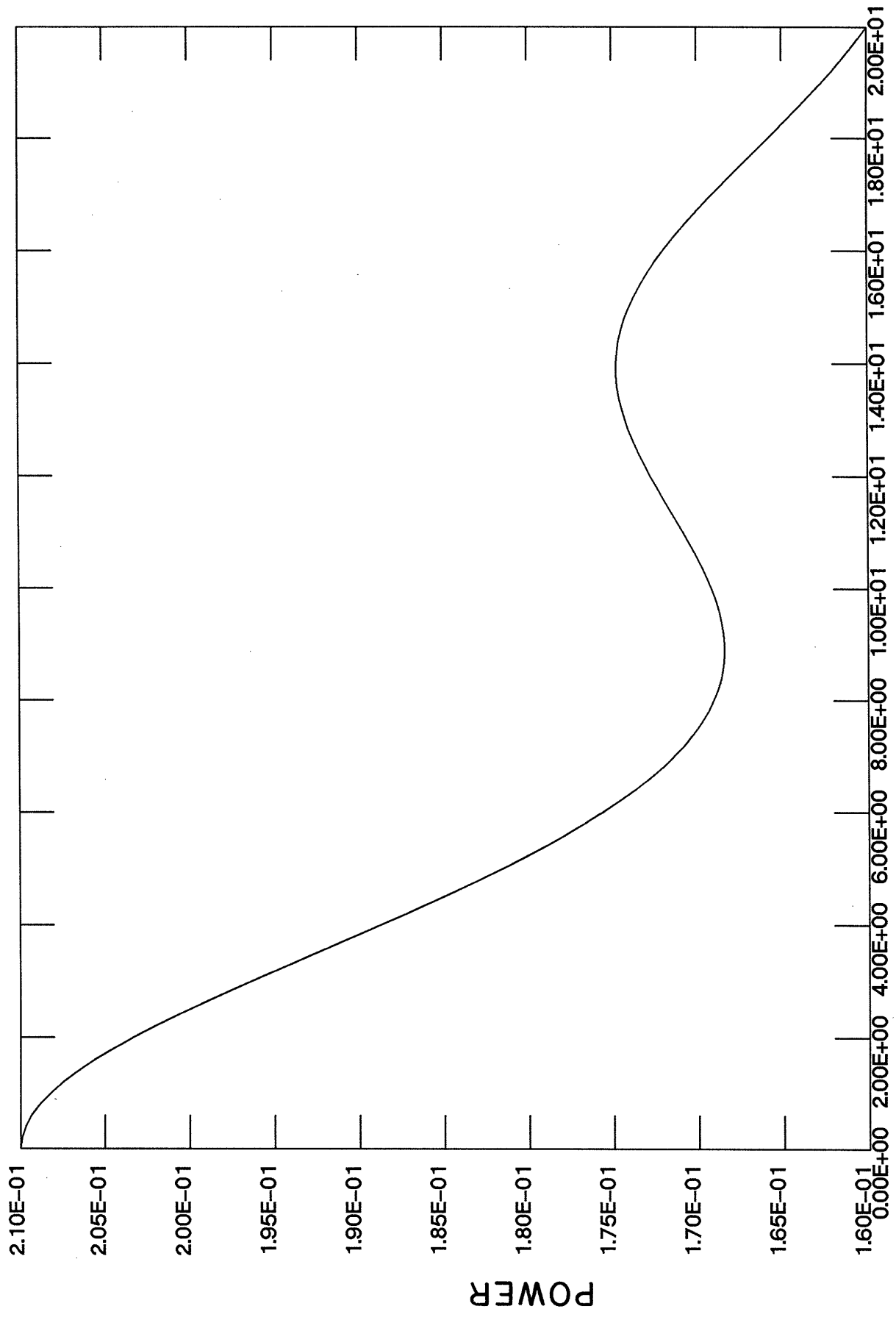
POWER
2.10E-01
2.05E-01
2.00E-01
1.95E-01
1.90E-01
1.85E-01
1.80E-01
1.75E-01
1.70E-01
1.65E-01
1.60E-01
0.00E+00
2.00E+00
4.00E+00
6.00E+00
8.00E+00
1.00E+01
1.20E+01
1.40E+01
1.60E+01
1.80E+01
2.00E+01
FREQUENCY (RAD/SEC)

Figure 7

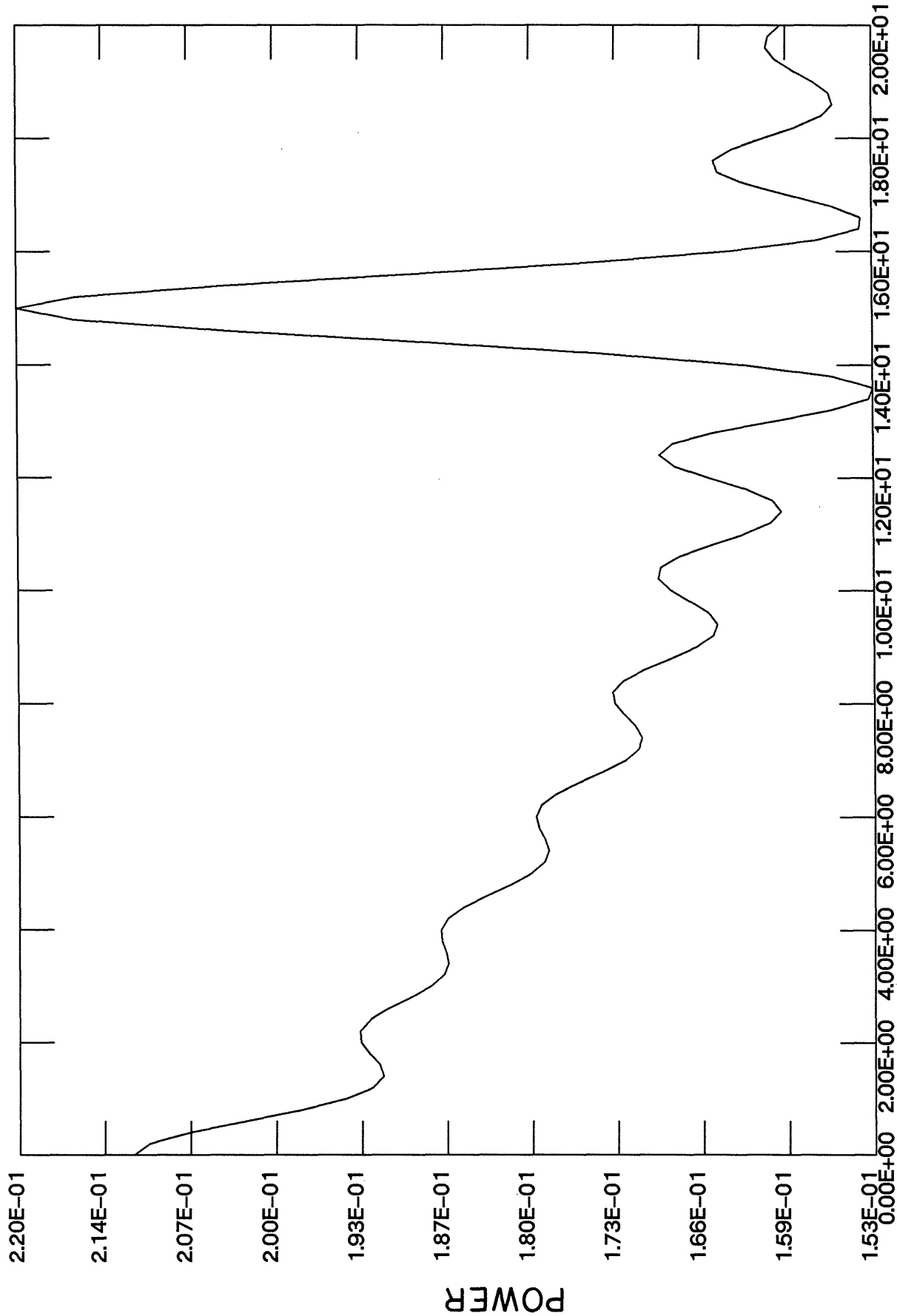
POWER
2.20E-01
2.14E-01
2.07E-01
2.00E-01
1.93E-01
1.87E-01
1.80E-01
1.73E-01
1.66E-01
1.59E-01
1.53E-01
0.00E+00
2.00E+00
4.00E+00
6.00E+00
8.00E+00
1.00E+01
1.20E+01
1.40E+01
1.60E+01
1.80E+01
2.00E+01
FREQUENCY (RAD/SEC)

Figure 8